Self-diffusion measurements in isotopic heterostructures of undoped and *in situ* doped ZnO: Zinc vacancy energetics

Alexander Azarov,[1,*] Vishnukanthan Venkatachalapathy,[1] Zengxia Mei,[2] Lishu Liu,[2] Xiaolong Du,[2] Augustinas Galeckas,[1] Edouard Monakhov,[1] Bengt G. Svensson,[1] and Andrej Kuznetsov[1,†]

[1] *University of Oslo, Department of Physics, Centre for Materials Science and Nanotechnology, PO Box 1048 Blindern, N-0316 Oslo, Norway*

[2] *Institute of Physics, The Chinese Academy of Sciences, Beijing 100190, China*

(Received 3 May 2016; revised manuscript received 17 October 2016; published 17 November 2016)

It is well established that formation energies of point defects depend on the chemical potential (μ) and Fermi level position (E_F), which is widely used when modeling diffusion phenomena in semiconductors. In return, Arrhenius analysis of self-diffusion can be exploited for the investigation of point defect energetics since self-diffusion is mediated by intrinsic point defects. Specifically, the energetics of Zn vacancies (V_{Zn}) and/or Zn interstitials in ZnO can be potentially revealed via Zn self-diffusion measurements. In this study we have measured Zn self-diffusion varying μ (by shifting from Zn- to O-rich conditions during the sample synthesis) and E_F (by Ga, F, and Cu *in situ* doping). Corresponding diffusion activation energies were deduced and are discussed in terms of the vacancy diffusion mechanism. This results in an upper limit estimate for the V_{Zn} migration energy of ~1.5 eV, and prominent trends for the V_{Zn} formation energy as a function of μ and E_F are revealed. Concurrently, it is argued that dopant-V_{Zn} clustering and E_F pinning at deep donor traps should be taken into account when generalizing the interpretation of diffusion data for impurities in ZnO.

DOI: 10.1103/PhysRevB.94.195208

I. INTRODUCTION

ZnO is a modern, or more correctly phrased, "rediscovered" semiconductor receiving remarkable interest on behalf of its unique fundamental properties [1] and promising technological applications [2]. However, in spite of large research efforts on ZnO (see, for example, review [3] and references therein), the understanding of point defects and defect complexes is still insufficient to resolve the issues limiting ZnO device processing. Specifically, one of the main challenges is the so-called "native" *n*-type conductivity, also referred to as the "doping asymmetry," where donor-type doping is readily achievable only [4]. The origin of this effect is still under debate and is commonly attributed to a number of reasons, including spontaneous formation of "intrinsic" donors such as oxygen vacancies (V_{O}) and/or Zn interstitials ($\mathrm{Zn_i}$) having sufficiently low formation energies [5,6]. Concurrently, it was demonstrated that promising acceptors of group-V elements exhibit nontrivial configurations in ZnO, particularly forming complexes with Zn vacancies (V_{Zn}), such as $\mathrm{X_{Zn}}$-$2V_{\mathrm{Zn}}$($\mathrm{X} = \mathrm{P, As, or\ Sb}$), instead of simplistically residing on oxygen sites [7]. Moreover, V_{Zn}, an acceptor in its isolated form, also forms complexes with donor impurities, e.g., $\mathrm{Ga_{Zn}}$ - V_{Zn} and $\mathrm{Al_{Zn}}$ - V_{Zn} complexes are shown to play prominent roles [8–11]. Thus, revealing the energetics of intrinsic primary defects in ZnO is of fundamental as well as practical interest.

Considerable progress in the understanding of point defects in ZnO on atomic scale is reached by applying *ab initio* methods deducing energetics of the defects, and their complexes, from total energy calculations [12,13]. In particular, it has been shown that the formation energy of the defects in ZnO depends on (i) the chemical potential (μ) varying from O- to Zn-rich growth limits, and (ii) the Fermi level position (E_F) [12,13]. Moreover, the consideration of intrinsic defect energetics in terms of (i) and (ii) is of universal validity and applicable to other semiconductors too [14]. However, experimental data to compare with the theoretical predictions are limited. Meanwhile, Arrhenius analysis of self-diffusion is a direct method probing intrinsic defect energetics as long as the atomic jumps are mediated by defects. Note that self-diffusion experiments have distinct advantages over the impurity diffusion, which can alter E_F in the course of the impurity redistribution and require additional assumptions [10]. However, even in the "simple" case of measuring self-diffusion occurring via the vacancy mechanism, the presence of impurities intentionally introduced to change E_F may provoke the formation of impurity-vacancy complexes, altering the defect balance from its "thermodynamic" value. In addition, E_F at the "diffusion" temperature can be "pinned" to the position of deep traps if they appear with high concentration.

The diffusion data for ZnO available in the literature are quite contradictory and there is a puzzling discrepancy for the Zn self-diffusion activation energy (${E^a}_{\mathrm{Zn}}$), ranging from 1.8 to 4.3 eV [15–21]. Accounting for these variations, Zn self-diffusion was simulated as a function of the μ and E_F [22] and resulted in reasonable fits to the literature data, admitting, however, a serious weakness—the fact that the actual μ and E_F values were unknown and used as fitting parameters. Overall, self-diffusion measurements utilizing isotopic tracers—demonstrated to be very successful resolving intrinsic defect issues in other semiconductors [23]—are insufficiently addressed for ZnO. Altogether, it works as a strong motivation to undertake a Zn self-diffusion experiment enabling discriminations between μ, E_F, and dopant-defect reaction effects.

[*] Corresponding author: aazarov@smn.uio.no

[†] Corresponding author: andrej.kuznetsov@fys.uio.no

  ©2016 American Physical Society

TABLE I. Identification of the samples used in the present study. The nominal dopant concentrations, activation energies ($E^a{}_{Zn}$) and prefactors (D_0) of Zn self-diffusion are given.

Sample	Synthesis condition	Dopant (cm^{-3})	$E^a{}_{Zn}$ (eV)	ln [D_0 ($cm^2\,s^{-1}$)]
Z	Zn rich	undoped	3.7 ± 0.1	2.3 ± 1.5
ZCu	Zn rich	[Cu] = 7×10^{18}	3.7 ± 0.2	2.1 ± 2
ZGa1	Zn rich	[Ga] = 3×10^{19}	2.85 ± 0.15	2.2 ± 1.8
ZGa2	Zn rich	[Ga] = 3×10^{20}	2.6 ± 0.15	0.8 ± 2.2
O	O rich	undoped	1.5 ± 0.1	-18.5 ± 2
OF	O rich	[F] = 3×10^{19}	1.55 ± 0.1[a]	-18 ± 2[a]

[a]For the sample OF, $E^a{}_{Zn}$ and D_0 are quoted only for the high temperature part of the experimental data.

II. EXPERIMENT

Isotopically modulated ZnO samples were synthesized at 600° C by radio frequency plasma assisted molecular beam epitaxy on *c*-oriented Al_2O_3 substrates [24]. Two sorts of Zn source were used in the synthesis: either in its natural isotopic form or artificially enriched up to 99.4% with ^{64}Zn. The samples were prepared in the form of double films, consisting of the natural ZnO layer (∼200–400 nm thick) grown on the top of the isotopically enriched one (∼600–800 nm thick). In order to vary μ, the samples were grown under two conditions, O or Zn rich, by changing the rate of the oxygen flow while keeping the zinc supply as well as the plasma power constant. In addition to the undoped samples, a part of the Zn-rich samples were uniformly *in situ* doped with Ga and Cu, while the O-rich ones were doped with F. Samples are labeled as XY with X = O or Z for O- or Zn-rich growth conditions, respectively, and Y = Ga, Cu, or F for the dopants used (note ZGa1 and ZGa2 label samples with different Ga content). See Table I for an overview of the samples studied.

All the anneals were performed in air at 650–1100° C using a conventional tube furnace [25]. Concentration versus depth profiles of the Zn isotopes and dopants were measured by secondary ion mass spectrometry (SIMS). The signal-to-concentration calibration was performed using ZnO samples assuming a natural abundance of the stable Zn isotopes. The conversion of the SIMS sputtering time to depth was performed by measuring the crater depth using a Dektak 8 stylus profilometer and assuming a constant erosion rate. The diffusion profiles were simulated using second Fick's law applying reflective boundary conditions with the as-grown profile as initial condition. The diffusion activation energies ($E^a{}_{Zn}$) were extracted with an accuracy of $\leqslant 0.2$ eV given by the scattering of the data.

The E_F positions, as reached in the samples at the actual diffusion temperatures, were estimated by input from the "extrinsic" electron concentrations at room temperature (RT) determined by Hall measurements after each annealing step. On the basis of these values, $E_F(T)$ was then calculated employing the classical semiconductor physics formalism omitting band-gap narrowing. In addition, for some selected samples $E_F(T)$ was measured in the temperature range of RT–550 °C, applying temperature-dependent Hall effect (TDH) measurements.

III. RESULTS AND DISCUSSION

Figure 1 illustrates the results of the diffusion measurements undertaken in the undoped samples prepared with different μ. Figure 1(a) confirms that Zn self-diffusion is consistent with Fick's formalism and Arrhenius plots are shown in Fig. 1(b). The Zn self-diffusion is strongly enhanced when changing from Zn- to O-rich growth condition, i.e., changing μ, resulting in $E^a{}_{Zn}$ of 3.7 and 1.5 eV, respectively. It should be underlined that this effect is not attributed to E_F variations because both samples exhibit nearly identical electron concentrations after annealing, as illustrated by the inset in Fig. 1(b). Notably, the difference between the two resulting $E^a{}_{Zn}$ values is nearly as large as the range of $E^a{}_{Zn}$ values quoted in the literature

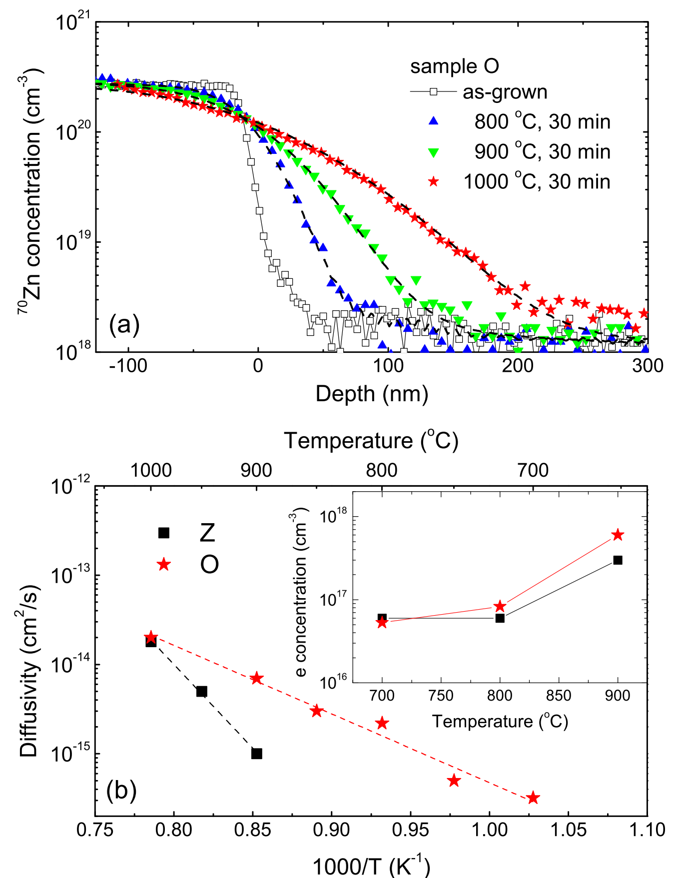

FIG. 1. (a) Concentration versus depth profiles of ^{70}Zn in the undoped O-rich isotopic heterostructures before and after anneals as indicated in the legend. Simulated depth profiles are shown by the dashed lines. (b) Arrhenius plots for Zn self-diffusion constants in the undoped Zn- and O-rich samples. The corresponding RT electron concentrations are shown in the inset in (b).

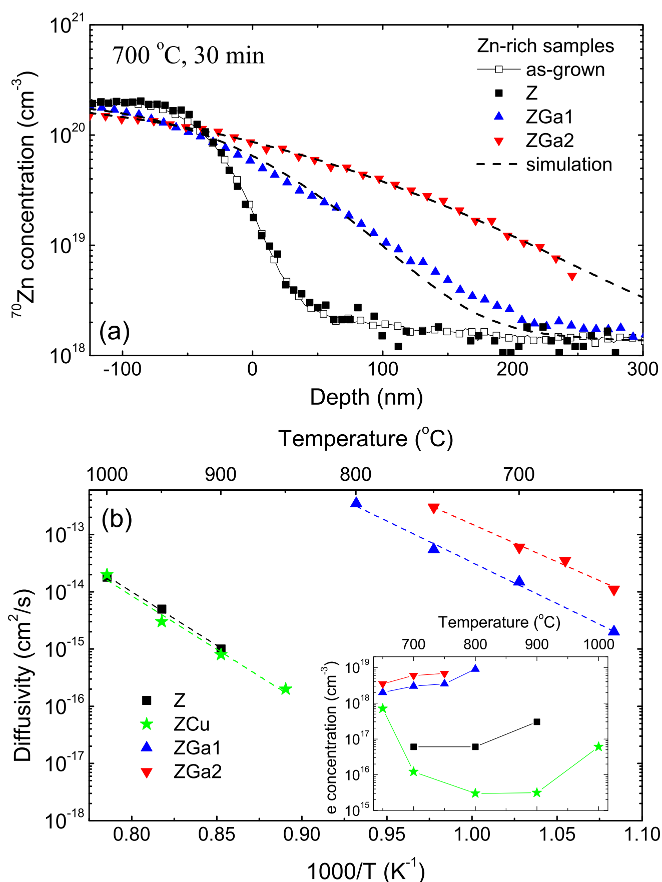

FIG. 2. (a) Concentration versus depth profiles of ^{70}Zn in the undoped and Ga doped isotopic heterostructures after 700 °C annealing illustrating an enhancement of Zn diffusion as a function of Ga content. (b) Arrhenius plots for Zn self-diffusion in the Cu- and Ga-doped Zn-rich samples. The corresponding room temperature electron concentrations are shown in the inset.

[15–21]. Previous experimental [19] and theoretical [12] studies indicate that Zn self-diffusion in n-type ZnO occurs primarily via the vacancy mechanism [26], which is fully corroborated by the data in Fig. 1(b). Therefore, using the conventional approach that $E^a{}_{\rm Zn}$ is composed of the formation (E^f) and migration (E^m) energies of $V_{\rm Zn}$, i.e., the defect predominantly mediating the diffusion [27], we can write $E^a{}_{\rm Zn} = E^f{}_{V\rm Zn} + E^m{}_{V\rm Zn}$, where $E^m{}_{V\rm Zn}$ is assumed to be unaffected by E_F and μ variations. Accordingly, $E^m{}_{V\rm Zn}$ should not exceed the lowest $E^a{}_{\rm Zn}$ obtained in our experiments, i.e., 1.5 eV is an upper limit for $E^m{}_{V\rm Zn}$. Furthermore, once $E^m{}_{V\rm Zn}$ is known it is possible to "translate" the self-diffusion activation energy into the vacancy formation energy via $E^f{}_{V\rm Zn} = E^a{}_{\rm Zn} - E^m{}_{V\rm Zn}$, yielding $E^f{}_{V\rm Zn} \geqslant 2.2$ eV in the undoped Zn-rich samples. In its turn, the theoretical estimations of $E^m{}_{V\rm Zn}$ give values around 1.4 eV [12] consistent with 1.5 eV being an upper limit. Note that a low value of $E^f{}_{V\rm Zn}$ in the O-rich samples is not surprising since theory predicts the formation energy of Zn vacancies for O-rich conditions could be close to zero for highly n-type doped materials [1].

Further exploration of the $E^f{}_{V\rm Zn}(E_F)$ can be done by analyzing Zn self-diffusion in intentionally doped samples. Figure 2(a) shows the results of the diffusion measurements undertaken in the Zn-rich samples at 700 °C, illustrating a clear trend of self-diffusion enhancement as a function of the Ga concentration. Indeed, at 700 °C the Zn atoms are practically immobile in the undoped material but remarkably mobile upon Ga doping. The inset in Fig. 2(b) summarizes the RT carrier concentration as a function of annealing temperature in Ga and Cu doped samples. Simplistically, $E^f{}_{V\rm Zn}$ and the corresponding $E^a{}_{\rm Zn}$ should decrease with E_F moving towards to the bottom of the conduction band E_C (Ga doping) and the opposite when shifting E_F towards midgap (Cu doping). Figure 2(b) shows the Arrhenius plots for Zn self-diffusion in these samples and $E^a{}_{\rm Zn}$ decreases to 2.85 and 2.6 eV in the ZGa1 and ZGa2 samples, respectively. In fact, this provides an additional argument in favor of the vacancy diffusion mechanism to mediate the Zn self-diffusion, because if $\rm Zn_i$ is involved, the trend for $E^a{}_{\rm Zn}(E_F)$ would be the opposite [12,13,22]. Nevertheless, there is a significant discrepancy between the chemical Ga contents (see Table I) and electron concentrations [the inset in Fig. 2(b)]. Despite that anneals enhance the Ga activation, it remains incomplete even after 800 °C, suggesting the presence of $\rm Ga_{Zn}$ - $V_{\rm Zn}$ acceptors in our samples [8,9]. Under this assumption, dissociation of the $\rm Ga_{Zn}$- $V_{\rm Zn}$ complexes may be at least partly responsible for releasing $V_{\rm Zn}$ and, as a result, enhancement the Zn self-diffusion. It should be noted that in the case of efficient dissociation of vacancy-dopant complexes a transient-enhanced diffusion could be expected. However, this effect should not play a pronounced role in the Ga doped samples because of a modest dissociation of Ga-related complexes [see the inset in Fig. 2(b) demonstrating only a minor increase of the electrical activation of Ga with temperature] at the annealing temperatures used in our experiments. In its turn, Fig. 2(b) shows that increasing Ga content leads to an almost parallel shift of the Arrhenius plot by a factor close to the difference in the Ga content for the samples ZGa1 and ZGa2. This may imply that, in addition to single $V_{\rm Zn}$'s, mobile $\rm Ga_{Zn}$ - $V_{\rm Zn}$ complexes may contribute to mediate Zn self-diffusion in the heavily doped samples.

In contrast, the Zn self-diffusion in the Cu-doped samples does not follow the $E^a{}_{\rm Zn}(E_F)$ trend. As a group-Ib element, Cu substituting Zn may be anticipated to act as an acceptor [28]. However, the as-grown Cu-doped samples show n-type conductivity with an electron concentration of $\sim 10^{18}$ cm^{-3} indicating that a large fraction of the Cu atoms is interstitial or forms donor type complexes. Annealing leads to a partial Cu-acceptor activation and, as a result, to a dramatic decrease in the electron concentration at RT [see the inset in Fig. 2(b)]. The estimated E_F position in the ZCu sample is about 0.3 eV lower than in the Z samples for the temperature range of 800–1000 °C (see Fig. 3). Such a strong decrease in E_F implies a dramatic increase of $E^f{}_{\rm Zn}$ and, therefore, a possible retardation of the Zn self-diffusivity. However, the Zn self-diffusivity in the ZCu and Z samples exhibits identical behavior in the whole temperature range with identical $E^a{}_{\rm Zn}$ and similar pre-exponential factors (Fig. 2 and Table I). This shows that the Cu doping does not cause any significant change in the free carrier concentration at the diffusion temperatures. Hence, Cu-related traps do not play a primary role. Instead the observed behavior can be attributed to pinning of E_F by deep trap(s). Possible generic candidates for the traps are the so-called $E3$ or $E4$ centers as indicated by the dashed lines in Fig. 3. $E3$ is a prominent

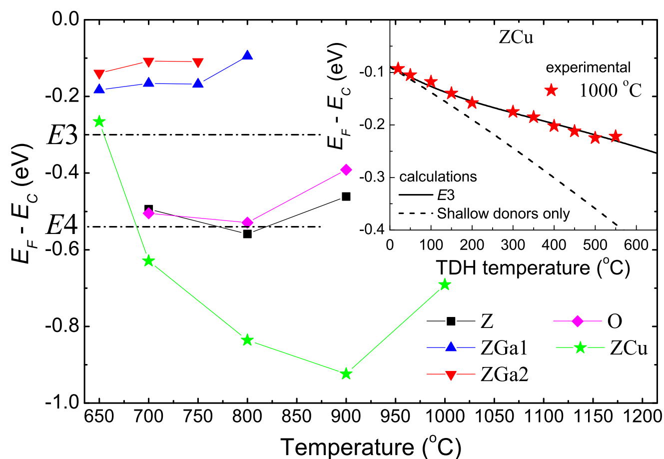

FIG. 3. Fermi level positions as a function of temperature in the range employed for diffusion. The positions of the so-called $E3$ and $E4$ levels (relative to the E_C) are indicated by the dash-dotted lines. The inset shows the Fermi level positions in the ZCu sample annealed at 1000 °C obtained from the TDH measurements (stars) in comparison with theoretically predicted ones assuming shallow donors only with a concentration of 7×10^{16} cm^{-3} (dashed line) and an additional deep $E3$ donors with a concentration of 2×10^{18} cm^{-3} (solid line).

and commonly observed donorlike state at E_C-0.3 eV, which occurs irrespective of the synthesis method used [29]. It has been suggested that $E3$ is related to a dual vacancy V_O-V_{Zn} [30], or Zn interstitials [31], but recently it was unambiguously shown that $E3$ involves hydrogen [32]. In its turn, the $E4$ level is located at $E_C - 0.54$ eV and could be attributed to a Zn-rich defect [33] or V_O [34].

The scenario of E_F pinning is also supported by the temperature dependence of E_F deduced from the TDH results, as illustrated by the inset in Fig. 3 showing data for the ZCu sample annealed at 1000 °C. In the deduction, we have assumed fully ionized shallow donors with a concentration of 7×10^{16} cm^{-3} at RT (corresponding to the electron concentration measured at RT). The theoretically predicted $E_F(T)$ in case of shallow donors only and in case of additional $E3$ centers with a concentration of 2×10^{18} cm^{-3}, are shown by the dashed and solid lines, respectively. The experimental $E_F(T)$ data are satisfactorily described by the latter assumption but not by the former one. Here it should be underlined that the value used for $E3$ concentration may contain contributions from several different deep donor centers and not only from $E3$ itself.

Figure 4 shows the obtained $E^f{}_{VZn}$ values versus E_F (deduced for the temperature range of diffusion) for all the samples studied. The potential shift in E_F for the ZCu sample due to pinning is indicated by the arrow. It should be noted that the deep donor states can also affect the E_F position in the undoped samples; however, this effect should be smaller as compared to the ZCu samples. In summary, the trend and the magnitude of $E^f{}_{VZn}$ corroborates the theoretical prediction of decreasing $E^f{}_{VZn}$ when E_F approaches E_C and when μ changes from Zn- to O-rich conditions [12,13,22]. Moreover, the slope of the $E^f{}_{VZn}(E_F)$ dependence (for a given μ) yields the charge state of V_{Zn}, and according to theory the double

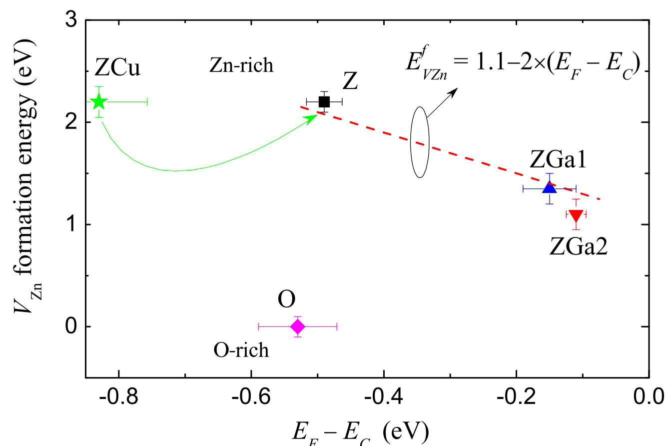

FIG. 4. Deduced formation energy of V_{Zn} versus Fermi level position (averaged over the temperature range of diffusion) in the samples studied. The dashed line illustrates the trend of $E^f{}_{VZn}$ versus E_F assuming a double negative charge state of V_{Zn} (see the text for details).

negative charge state of V_{Zn} should dominate in our samples [12]. Indeed, linear fitting of the data for the Zn-rich samples (shown by the thick dashed line in Fig. 4) suggests $V_{Zn}{}^{2-}$ as the mediating defect [35].

The E_F position can also be tuned by doping with donors substituting oxygen such as F (F_O). In contrast to Ga, nearly complete dopant activation is obtained in the as-grown F-doped sample (see the inset in Fig. 5 showing the RT electron concentration and F content as a function of the annealing temperature for the OF samples). At high temperatures the Zn self-diffusion in the OF samples resembles that in the O samples correlating with the loss of F from the samples (see the inset in Fig. 5). Intriguingly, a strong retardation in the Zn self-diffusion [36] at low temperatures occurs when the F and electron concentrations are still high, and E_F is most

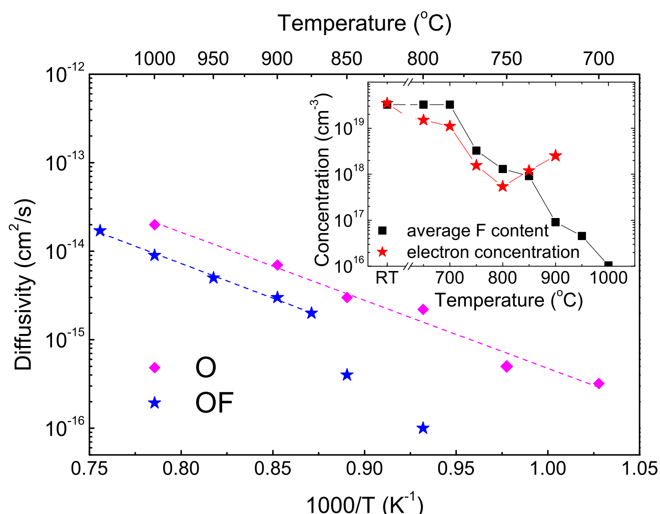

FIG. 5. Arrhenius plots of the extracted Zn self-diffusion constants vs the reciprocal absolute temperature in the undoped and F-doped O-rich samples. The corresponding RT electron concentrations and retained F content are shown in the inset.

likely situated at a similar position as in the ZGa2 samples. On the other hand, the concentration of mediating (free) $V_{Zn}{}'s$ should be low, and it is tempting to suggest that V_{Zn} forms stable acceptorlike complexes with F_O,F_O- V_{Zn}, promoted by the Coulomb interaction. The corresponding complexes for the Ga_{Zn} and Al_{Zn} donors (Ga_{Zn}-V_{Zn} and Al_{Zn}-V_{Zn}) have a dissociation energy of ∼1.9eV [37] and are not stable above ∼250° C. Notably, the formation of such F_O-V_{Zn} complexes may also be supported by the decreasing electron concentration relative to the F content already after the annealing at 650 °C, as seen from the inset in Fig. 5.

IV. CONCLUSIONS

In conclusion, migration and formation energies of V_{Zn} in ZnO are estimated from Zn self-diffusion experiments and an upper limit for $E^m{}_{VZn}$ of ∼1.5 eV is experimentally obtained. A striking correlation between our experimental data and previously reported theoretical results is demonstrated for $E^f{}_{VZn}(E_F,\mu)$. However, the effect of the E_F position on $E^f{}_{VZn}$ can be obscured by dopant-defect reactions affecting the point defect balance, and possible E_F pinning at deep donor states. In particular, Zn self-diffusion is strongly accelerated in Ga-doped samples, while F doping leads to retardation despite that both Ga and F exhibit shallow donor behavior. This apparent contradiction is discussed in terms of formation/dissociation of donor-acceptor pairs, like (F_O-V_{Zn}) and (Ga_{Zn}-V_{Zn}), suppressing or promoting the concentration of free (diffusion-mediating) V_{Zn} in F and Ga doped samples, respectively. In its turn, Cu doping does not affect Zn self-diffusion in spite of a pronounced decrease in the electron concentration, indicating E_F pinning by prominent deep level defects such as the $E3$ or $E4$ centers.

ACKNOWLEDGMENTS

Financial support from the Research Council of Norway (RCN) in the framework of the IDEAS (Project No. 221668) and the MIDAS (Project No. 228578) grant programs administrated via the ENERGIX program, and the National Natural Science Foundation of China (Grants No. 11274366, No. 51272280, No. 11674405, and No. 11675280) are gratefully acknowledged. A.A. acknowledges support from "The Norwegian Research Centre for Solar Cell Technology" and the RCN FRINATEK program.

[1] A. Janotti and C. G. Van de Walle, Rep. Prog. Phys. **72**, 126501 (2009).

[2] C. W. Litton, T. C. Collins, and D. C. Reynolds, *Zinc Oxide Materials for Electronic and Optoelectronic Device Applications* (John Wiley and Sons, New York, 2011).

[3] M. D. McCluskey and S. J. Jokela, J. Appl. Phys. **106**, 071101 (2009).

[4] S. B. Zhang, S.-H. Wei, and A. Zunger, Phys. Rev. B **63**, 075205 (2001).

[5] V. Avrutin, D. J. Silversmith, and H. Morkoç, IEEE **98**, 1269 (2010).

[6] L. Liu, Z. Mei, A. Tang, A. Azarov, A. Kuznetsov, Q.-K. Xue, and X. Du, Phys. Rev. B **93**, 235305 (2016).

[7] S. Limpijumnong, S. B. Zhang, S.-H. Wei, and C. H. Park, Phys. Rev. Lett. **92**, 155504 (2004).

[8] D. O. Demchenko, B. Earles, H. Y. Liu, V. Avrutin, N. Izyumskaya, Ü. Özgür, and H. Morkoç, Phys. Rev. B **84**, 075201 (2011).

[9] D. Steiauf, J. L. Lyons, A. Janotti, and C. G. Van de Walle, APL Mater. **2**, 096101 (2014).

[10] K. M. Johansen, L. Vines, T. S. Bjørheim, R. Schifano, and B. G. Svensson, Phys. Rev. Appl. **3**, 024003 (2015).

[11] J. E. Stehr, K. M. Johansen, T. S. Bjørheim, L. Vines, B. G. Svensson, W. M. Chen, and I. A. Buyanova, Phys. Rev. Appl. **2**, 021001 (2014).

[12] A. Janotti and C. G. Van de Walle, Phys. Rev. B **76**, 165202 (2007).

[13] S. Lany and A. Zunger, Phys. Rev. B **81**, 113201 (2010).

[14] S. B. Zhang and J. E. Northrup, Phys. Rev. Lett. **67**, 2339 (1991).

[15] W. J. Moore and E. L. Williams, Discuss. Faraday Soc. **28**, 86 (1959).

[16] J. J. Lander, J. Phys. Chem. Solids **15**, 324 (1960).

[17] D. G. Thomas, J. Phys. Chem. Solids **3**, 229 (1957).

[18] B. J. Wuensch and H. L. Tuller, J. Phys. Chem. Solids **55**, 975 (1994).

[19] G. W. Tomlins, J. L. Routbort, and T. O. Mason, J. Appl. Phys. **87**, 117 (2000).

[20] M. A. N. Nogueira, W. B. Ferraz, and A. C. S. Sabioni, Mat. Res. **6**, 167 (2003).

[21] K. Watanabe, K. Matsumoto, Y. Adachi, T. Ohgaki, T. Nakagawa, N. Ohashi, H. Haneda, and I. Sakaguchi, Sol. State Comm. **152**, 1917 (2012).

[22] P. Erhart, and K. Albe, Appl. Phys. Lett. **88**, 201918 (2006).

[23] H. Bracht, S. P. Nicols, W. Walukiewicz, J. P. Silveira, F. Briones, and E. E. Haller, Nature (London) **408**, 69 (2000).

[24] H. Kato, K. Miyamoto, M. Sano, and T. Yao, Appl. Phys. Lett. **84**, 4562 (2004).

[25] It should be noted that annealing ambient can potentially affect the balance of point defects in the bulk of the material. However, this phenomenon is more pronounced for annealing in vacuum as well as oxygen lean atmospheres. In its turn, anneals performed in air, i.e., oxygen containing ambient, proved to result in minor surface modifications, at least for temperatures <1000 °C [see, e.g., T. M. Børseth *et al.*, Phys. Scr. **T126**, 10 (2006)], which is of most interest for the present experiment.

[26] It should be mentioned that the obtained values of D_0 for the all Zn-rich samples are in the range of 2–10, which is consistent with theoretical predictions for a vacancy assisted diffusion mechanism [C. Zener, J. Appl. Phys. **22**, 372 (1951)]. In contrast, the D_0 values for the O-rich samples are unphysically low indicating limited validity of the extrapolation of the Arrhenius plots to high temperatures.

[27] J. Philibert, *Atom Movements: Diffusion and Mass Transport in Solids* (Les Editions de Physique, Paris, 1991).

[28] Y. Yan, M. M. Al-Jassim, and S.-H. Wei, Appl. Phys. Lett. **89**, 181912 (2006).

[29] F. D. Auret, S. A. Goodman, M. Hayes, M. J. Legodi, H. A. Van Laarhoven, and D. C. Look, Appl. Phys. Lett. **79**, 3074 (2001).
[30] G. Chicot, J. Pernot, J.-L. Santailler, C. Chevalier, C. Granier, P. Ferret, A. Ribeaud, G. Feuillet, and P. Muret, Phys. Status Solidi B **251**, 206 (2014).
[31] H. Frenzel, H. v. Wenckstern, A. Weber, H. Schmidt, G. Biehne, H. Hochmuth, M. Lorenz, and M. Grundmann, Phys. Rev. B **76**, 035214 (2007).
[32] A. Hupfer, C. Bhoodoo, L. Vines, and B. G. Svensson, Appl. Phys. Lett. **104**, 092111 (2014).
[33] V. Quemener, L. Vines, E. V. Monakhov, and B. G. Svensson, Appl. Phys. Lett. **100**, 112108 (2012).
[34] T. Frank, G. Pens, R. Tena-Zaera, J. Zúñiga-Pérez, C. Martínez-Tomás, V. Muñoz-Sanjosé, T. Ohshima, H. Itoh, D. Hofmann, D. Pfisterer, J. Sann, and B. Meyer, Appl. Phys. A **88**, 141 (2007).
[35] It should be noted that it is possible to obtain a charge state of the mediating defect using Fair's diffusion model (under the assumption that the model is valid) [see R. B. Fair and J. C. C. Tsai, J. Electrochem. Soc. **124**, 1107 (1977)]. However, we still have to use the free electron concentrations obtained by the Hall measurements performed at RT. So, there is no principle difference between the method based on Fair's diffusion model and the one used in the present paper.
[36] Note that the diffusivities shown for the OF sample were extracted after 30 min anneals assuming constant diffusivity without taking into account a decrease in the F content with annealing time.
[37] J. E. Stehr, W. M. Chen, B. G. Svensson, and I. A. Buyanova, J. Appl. Phys. **119**, 105702 (2016).